JMEPEG (2005) 14:722-727
DOI: 10.1361/105994905X75510

1059-9495/$19.00

Characterization of the α Phase Nucleation in a Two-Phase Metastable β Titanium Alloy

A. Lenain, N. Clément, M. Véron, and P.J. Jacques

(Submitted August 24, 2005)

Beta titanium alloys are increasingly the best choice for automotive and aerospace applications due to their high performance-to-density ratio. Among these alloys, the TIMETAL Ti-LCB is already used in the automotive industry because it presents excellent mechanical properties and a lower cost compared with other Ti alloys. The current study deals with the characterization of the nucleation and growth of the α phase in several thermomechanical processes, because the distribution and size of the α phase strongly influence the mechanical properties of the resulting microstructures. Several heat treatments were conducted after either cold rolling or annealing. The resulting microstructures were characterized by scanning electron microscopy, transmission electron microscopy, x-ray diffraction, or electron backscatter diffraction. It was observed that the morphology and the volume fraction of the α phase are strongly dependent on the holding temperature, on the heating or cooling rate, and on the β grain size.

Keywords α nucleation, β titanium alloy, microstructure, Ti LCB

1. Introduction

Titanium alloys are used more and more for structural applications, mainly in the automotive and aerospace industries. Thanks to their high performance-to-density ratio, Ti alloys can bring about a reduction in weight of 40% while presenting comparable mechanical properties to some grades of steel. Furthermore, metastable β grades present higher specific strengths than other α or α + β grades. They also exhibit excellent hardenability, cold deformability, and corrosion resistance (Ref 1).

The aerospace industry is interested in these grades because they can be good candidates for several parts of the low-pressure compressor of turboengines (Ref 2). One of the critical design parameters of these parts is the fatigue resistance under the regimes of both high-cycle fatigue (HCF) and low-cycle fatigue. More precisely, in the HCF regimen the critical parameter is the resistance to crack initiation under cycling loading.

It is well documented that the final mechanical properties, particularly the fatigue resistance, are strongly influenced by several characteristics of the microstructure like grain size, grain morphology, phase volume fraction, grain orientation, and grain misorientation (Ref 2-4). Continuous α films at the β grain boundaries can be deleterious for the mechanical properties (Ref 1, 5, 6) and must then be avoided by appropriate heat or thermomechanical treatments. As a consequence, the characterization and understanding of the precipitation sequence of the α phase as a function of the β prior grain size, the holding temperature, and the heating or cooling rates are of primary importance. It is, therefore, the purpose of the current study to assess the nucleation and growth sequence of the α phase during several thermomechanical treatments of Ti-LCB.

This paper was presented at the Beta Titanium Alloys of the 00's Symposium sponsored by the Titanium Committee of TMS, held during the 2005 TMS Annual Meeting & Exhibition, February 13-16, 2005 in San Francisco, CA.

A. Lenain, N. Clément, and **P.J. Jacques,** Université Catholique de Louvain, Département des Sciences des Matériaux et des Procédés, Unité d'Ingénierie des Matériaux et des Procédés (IMAP), Place Sainte Barbe 2, B-1348 Louvain-la-Neuve, Belgium; and **M. Véron,** Laboratoire de Thermodynamique et Physicochimie Métallurgiques (LTPCM), Centre National de la Recherche Scientifique (CNRS) 5614, 1130 Rue de la Piscine, BP75 F-38402 Saint Martin d'Hères, France. Contact e-mail: lenain@imap.ucl.ac.be.

2. Material and Experimental Procedure

The alloy was received from TIMET-Savoie as hot-rolled rods that are 12 mm in diameter. Its chemical composition is given in Table 1. The mean β transus temperature ($T\beta$) was determined by metallography and x-ray diffraction as 805 °C ± 5 °C.

To generate different microstructures, several heat or thermomechanical treatments were designed. These treatments are summarized in Fig. 1. To observe the influence of the β prior grain size on α nucleation, the samples were first solution-treated either at 810 °C for 5 min or at 850 °C for 1 h with a heating rate of about 10 °C/s. These conditions bring about grain sizes of 20 and 200 μm, respectively. They were then water quenched at a cooling rate of about 250 °C/s to room temperature and then reheated to the isothermal aging temperature, directly transferred to a bath at a lower temperature, or continuously cooled. The isothermal aging below the β transus

Table 1 Chemical composition of the investigated alloy

	Elements, wt.%						
Alloy	**Ti**	**Mo**	**Fe**	**Al**	**O**	**N**	**C**
Ti-LCB	Bal.	6.46	4.26	1.47	0.21	0.008	0.07

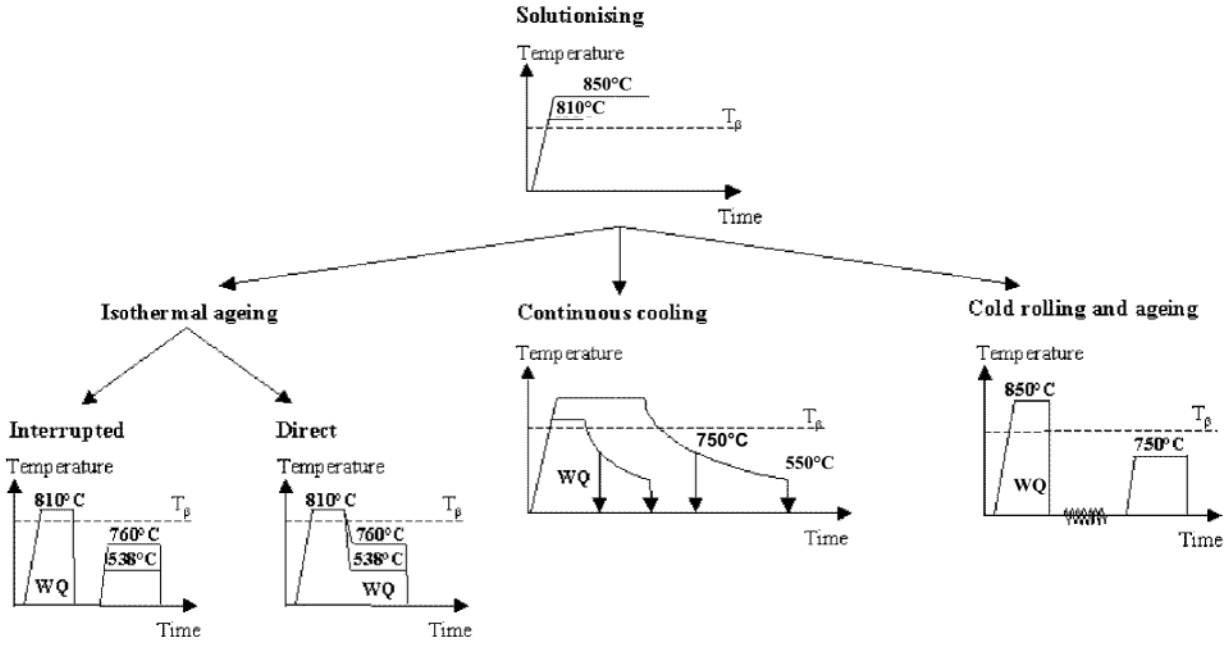

Fig. 1 Schematic illustration of the different heat treatments: (a) interrupted isothermal aging, (b) direct isothermal aging, (c) continuous cooling, (d) cold rolling and aging

was conducted at 760 °C for 30 min or at 538 °C for 6 h. In the case of continuous cooling, the cooling rate was 2 °C/min, and the samples were water-quenched from 750 and 550 °C to observe the evolution of the α nucleation and growth.

Finally, to favor the intragranular precipitation of the α phase at the expense of the continuous films at the prior β grain boundaries, several specimens were cold rolled after processing in solution and then were annealed at several temperatures for different times to activate the α precipitation and/or the β recrystallization (Fig. 1d).

To reveal the microstructures for light microscopy and scanning electron microscopy (SEM) observations, the specimens were first polished with diamond paste down to 0.25 μm and then were etched with a 10% HF-5% HNO_3 solution for times varying from 1 s to 1 min. Electron backscatter diffraction (EBSD) and orientation imaging microscopy (OIM) were also used to characterize the microstructures. In this case, polishing for 4 h with a colloidal silica suspension was carried out as the final polishing step. Observations were performed using a field emission scanning electron microscope (FEG-SEM) operating at 20 kV. Step size, ranging from 0.1 to 0.05 μm, was used. For transmission electron microscopy (TEM) observations, samples were thinned either by ion beam milling (for the two-phase microstructures) at an incident angle of 10 °C and an accelerating voltage of 4 kV, or by electropolishing (for the single phase microstructures) in an electrolyte comprising 95 vol.% of acetic acid and 5 vol.% of perchloric acid at 14 °C and a voltage of 22 to 25 V. The transmission electron microscope operated at 300 kV.

3. Results

The microstructure shown in Fig. 2(a) corresponds to the specimen placed in solution at 810 °C for 5 min, water-quenched, and reheated to 760 °C for 30 min. The α grains (the etched phase) are located both at the prior β grain boundaries and within the β grains. Furthermore, they are quite fine (~1 μm). For the sake of comparison, Fig. 2(b) shows the microstructure corresponding to the specimen aged at 760 °C for 30 min directly after treatment in solution at 810 °C. The volume fraction of the α phase is significantly smaller than in the case of the interrupted aging. The α phase can be found only at some places on the β grain boundaries.

The EBSD band contrast map corresponding to the microstructure of Fig. 2(a) is given in Fig. 3. It can be seen that the continuous film of α at the β grain boundaries results either from the coalescence of several grains or from only one α grain. Furthermore, a preferential growth along the prior β grain boundaries is observed.

The orientation relationship between α and β was determined for the α grains located at the β grain boundary on Fig. 3. In agreement with the literature (Ref 7), the Burgers relationship ($\{110\}_\beta // \{0001\}_\alpha$ and $\langle 111\rangle_\beta // \langle 11\bar{2}0\rangle_\alpha$) is observed. However, this relationship is obeyed randomly with one of the adjacent β grains without any apparent rule.

Figure 4 presents the microstructures corresponding to interrupted or direct aging at 538 °C for 6 h after treatment in solution at 810 °C. These microstructures are much finer than that for aging at 760 °C. Etching revealed a very fine structure within the β grains. In the present case, the α phase grew as very fine platelets oriented in well-defined directions in each β grain. The α phase is also present as a continuous film at the β grain boundaries. Furthermore, for this aging temperature, there is no major difference between the two types of treatments.

The microstructures obtained after continuous cooling interrupted are given at 750 °C (Fig. 5a) and 550 °C (Fig. 5b). At 750 °C, the α phase has nucleated at the grain boundaries and within the β grain as small platelets. These seem to coalesce at

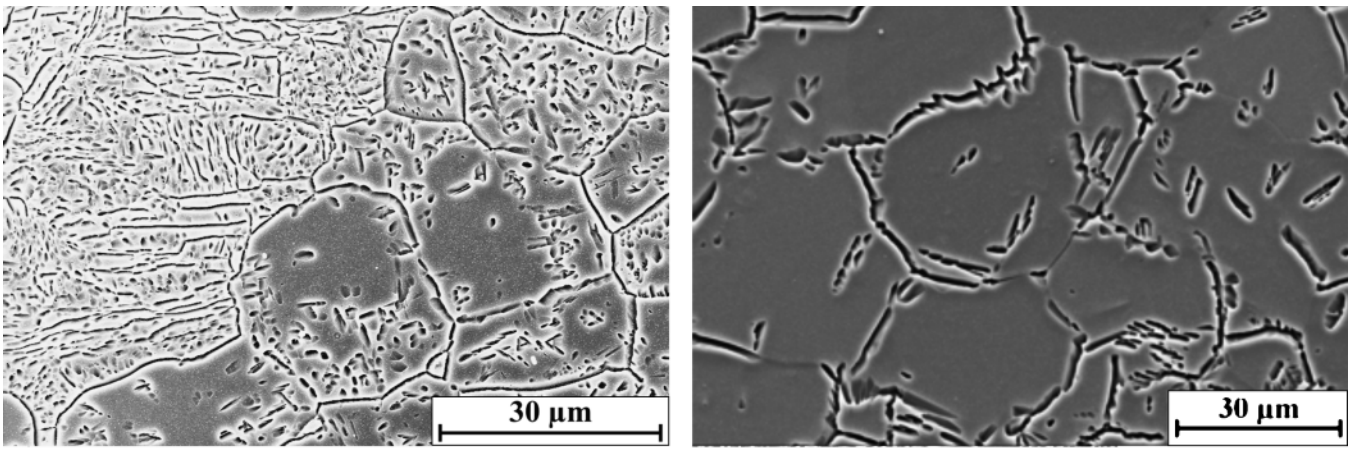

Fig. 2 Microstructures obtained by (a) interrupted aging at 760 °C for 30 min, (b) direct aging at 760 °C for 30 min, after the treatment in solution at 810 °C for 5 min

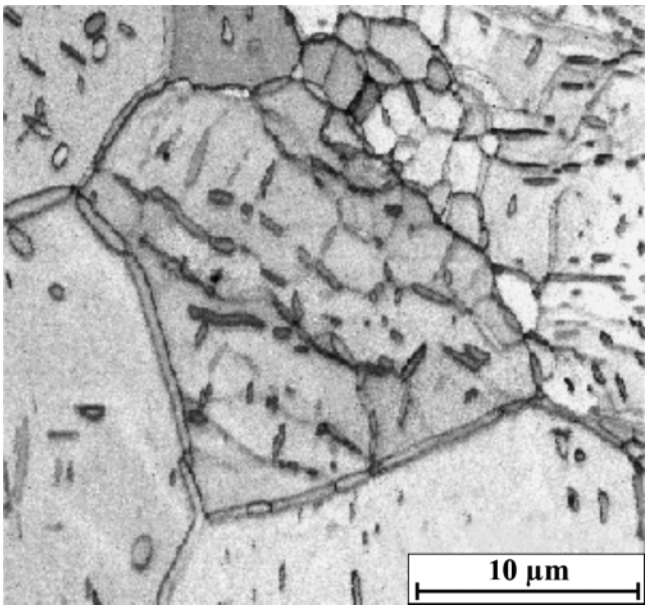

Fig. 3 EBSD map of the microstructure of Fig. 2(a)

several places. At 550 °C, a second population of finer platelets of α can be found between the larger platelets already observed at 750 °C.

Figure 6 corresponds to the microstructures obtained after treatment in solution at 850 °C for 1 h and continuous cooling stopped at 750 °C (Fig. 6a) and 550 °C (Fig. 6b). The volume fraction and the morphology of the α phase are very different than those in the case of continuous cooling from 810 °C. At 750 °C, the α phase is more heterogeneously distributed and can be mainly found close to the β grain boundaries. From a continuous film along the grain boundaries, some α platelets with well-defined orientations grew through the β grains. At 550 °C, the α phase also nucleated and grew within the β grains as a second population of finer α platelets.

The typical microstructure of the specimen that is cold rolled and annealed, as sketched in Fig. 1(d), is presented in Fig. 7. Very fine grains of α are uniformly distributed within the microstructure. However, the β phase did not recrystallize, as illustrated by the elongated shape of the grains.

As shown in Fig. 8, TEM observations reveal the presence of the nanometer ω phase within the β phase. Figure 8(b) shows that this last phase has a size of approximately 5 nm. This phase can be observed after direct quenching from above the β transus or after aging at lower temperatures. It is, thus, worth noting that all of the microstructures are characterized by the presence of three phases (i.e., α, β, and ω).

4. Discussion

The parameters of the heat treatment influence several features of the α phase that forms from the β grains after either cooling down from above the β transus or reheating from room temperature. The volume fraction, distribution, size, and morphology of the α grains can vary in a large way.

It is well known that the volume fraction of the precipitated α phase depends on aging temperature and time, respectively. Using MTDATA, the equilibrium volume fraction of α has been calculated for the Ti-LCB. At 750 °C, 20% of α should be present, and 55% at 550 °C. Some of the microstructures present such a proportion of α and β. This is the case for the continuously cooled specimens (i.e., the specimens aged at 538 °C or the specimen interruptedly aged at 760 °C). However, a large difference can be observed for the directly aged specimen at 760 °C, enlightening the influence of the nucleation stage.

According to the literature (Ref 8, 9), two regimes of temperatures can be distinguished. At a high temperature, around 750 °C, the decomposition of the β phase is principally characterized by the precipitation of the α phase at the grain boundaries, while at lower temperatures (~550 °C) intragranular α precipitation is reported.

For the high temperatures, a continuous film is observed in Fig. 2. Furthermore, as shown in Fig. 3, this film can result from the coalescence of several α precipitates that nucleated independently because the Burgers orientation relationship is followed randomly with one or the other β grains. The continuously cooled specimen down to 750 °C also presents such a continuous film of α. However, it is quite surprising that the specimen that is directly aged at 760 °C (Fig. 2b) presents a much smaller amount of α than this continuously cooled specimen, while both specimens spent the same time at or above 750 °C.

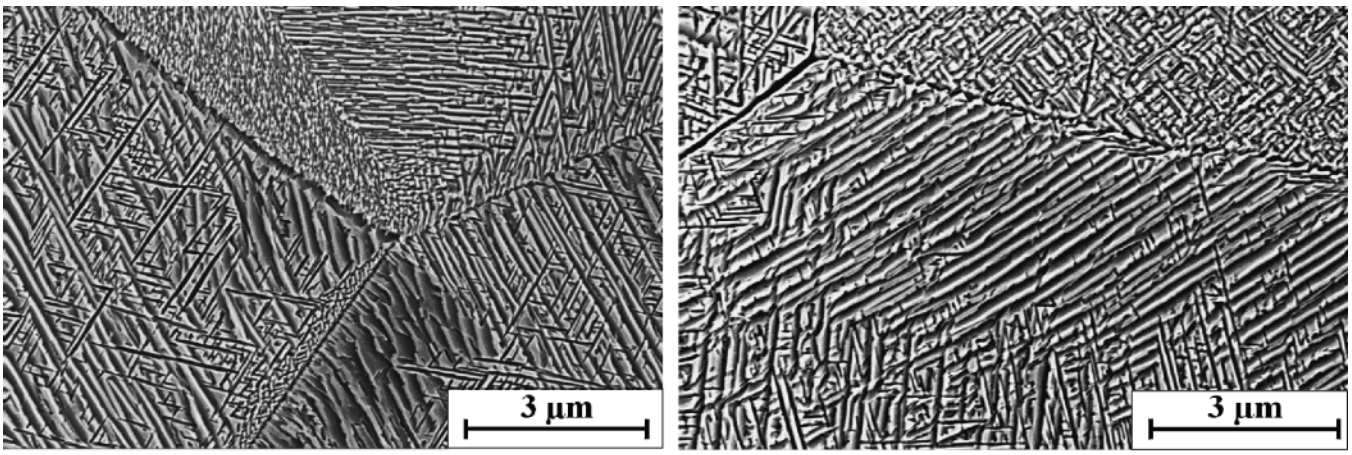

Fig. 4 Microstructures obtained by (a) interrupted aging and (b) direct aging at 538 °C for 6 h, after the treatment in solution at 810 °C for 5 min

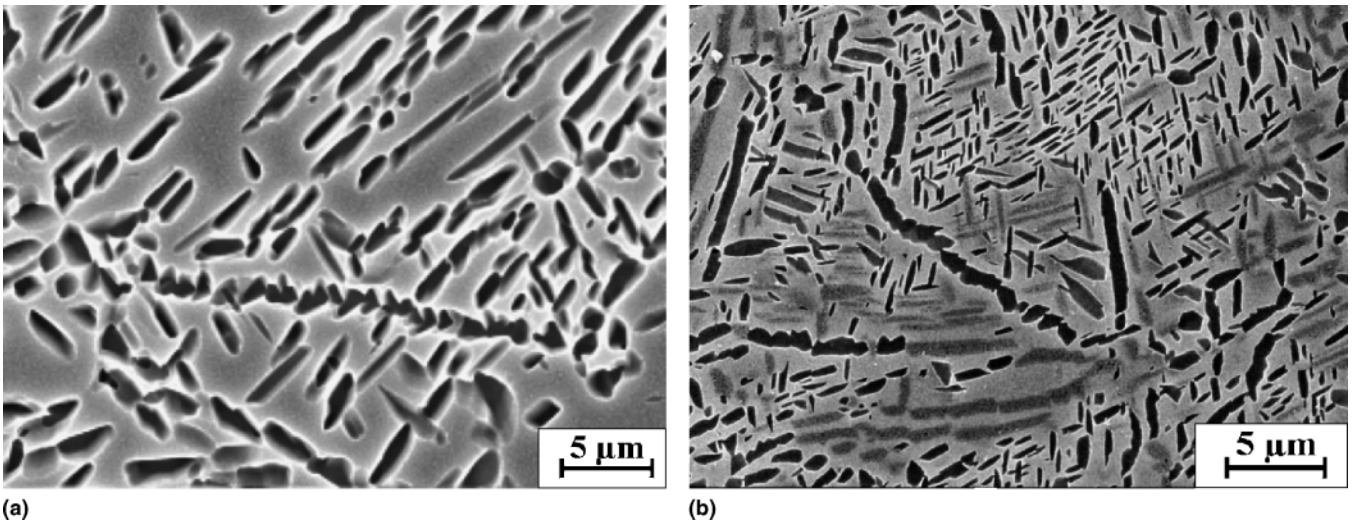

Fig. 5 Microstructures obtained by quenching from (a) 750 °C or (b) 550 °C after continuous cooling from 810 °C at 2 °C/min

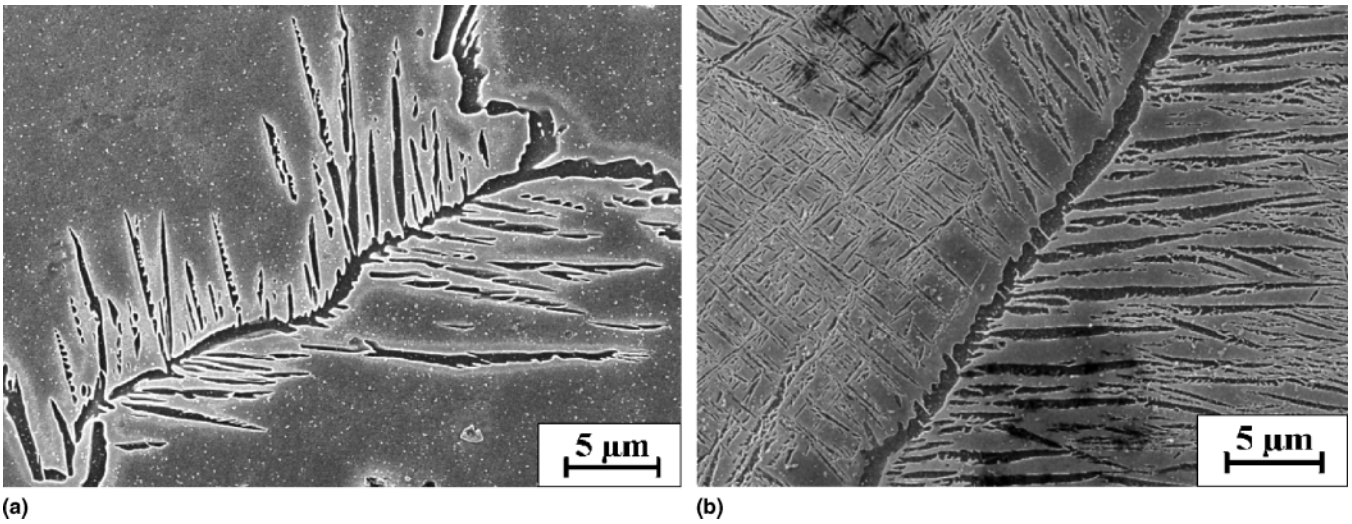

Fig. 6 Microstructures obtained by quenching from (a) 750 °C or (b) 550 °C after continuous cooling from 850 °C at 2 °C/min

Nevertheless, an intragranular precipitation of the α phase is observed in the case of the interrupted aging at 760 °C (Fig. 2a). It can be postulated, in agreement with the literature (Ref 1), that the quenching to room temperature brings about the formation of precursors that accelerate the nucleation rate of the α phase. These precursors can be dislocations resulting from the thermal stresses during quenching or metastable ω particles that are present in the Ti-LCB, as shown in Fig. 8. This phase forms spontaneously during quenching below a well-defined temperature (defined by the ω start temperature [ω^s]) through an athermal, displacive mechanism (Ref 8). This temperature is around 350 °C for the Ti LCB (Ref 8, 9). Prima et al. (Ref 10) have shown that the reversal transformation of ω to β during heating from room temperature generates some defects in the β matrix that can facilitate the α nucleation. It is worth noting that the influence of the heating rate on the formation of the α phase should, thus, be elucidated.

The beneficial influence of defects on the α nucleation can also be observed in Fig. 7. The dislocations resulting from the cold-rolling stage seem to promote the intragranular nucleation of α grains, leading to a very fine distribution of α grains within the β matrix. However, this precipitation seems to hinder the β recrystallization. As shown by Ivasishin et al. (Ref 11), the presence of some α grains completely hinders the β recrystallization. Because the β phase is quite far from equilibrium after quenching, the driving force for the α nucleation during heating is larger than the driving force for the β recrystallization. It can be postulated that the α nucleation depletes the potential sites for the β recrystallization.

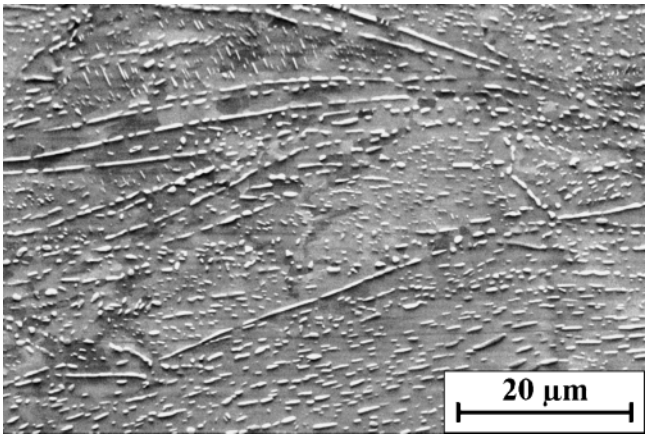

Fig. 7 Band contrast map of the microstructure of the specimen annealed at 750 °C for 15 min after cold rolling of the β phase

The second temperature range, at around 550 °C, is characterized by the decomposition of the β phase as a thin continuous α film at the grain boundaries, followed by the intragranular α precipitation as fine platelets. Due to a high nucleation rate, the microstructure is much finer. It is worth noting that these platelets can be too small to deform plastically, thus acting as hard, undeformable particles (Ref 1). The difference with holding at high temperature is that the interface of the platelets formed at 538 °C seems to be flat. Malinov et al. (Ref 12) showed that at approximately 500 °C the complete $\beta \rightarrow \beta + \alpha$ transformation necessitates much more time than at a higher temperature. They explained this phenomenon by the fact that, in this temperature range, the $\beta \rightarrow \beta + \alpha$ phase transformation is mainly controlled by the diffusion of molybdenum within the β phase.

Finally, another important parameter is the prior β grain size, which depends on the temperature of the solution treatment and time. Gil et al. (Ref 13) showed that a larger β grain size leads to a smaller width for the α plates. Our results are in agreement with those of this study, as shown in Fig. 5 and 6. However, these figures tend to show that the inverse trend prevails for the length of the platelets. Furthermore, Fig. 5 and 6 also show that the volume fraction of the α phase is higher in the case of the solution treatment at 810 °C than that at 850 °C. This difference results from the decrease of the starting temperature of the $\beta \rightarrow \alpha$ transformation with the increase of the β grain size. Indeed, an increase of the β grain size leads to a decrease of the β grain boundary surface area per unit volume and, thus, to fewer nucleation sites for the α phase.

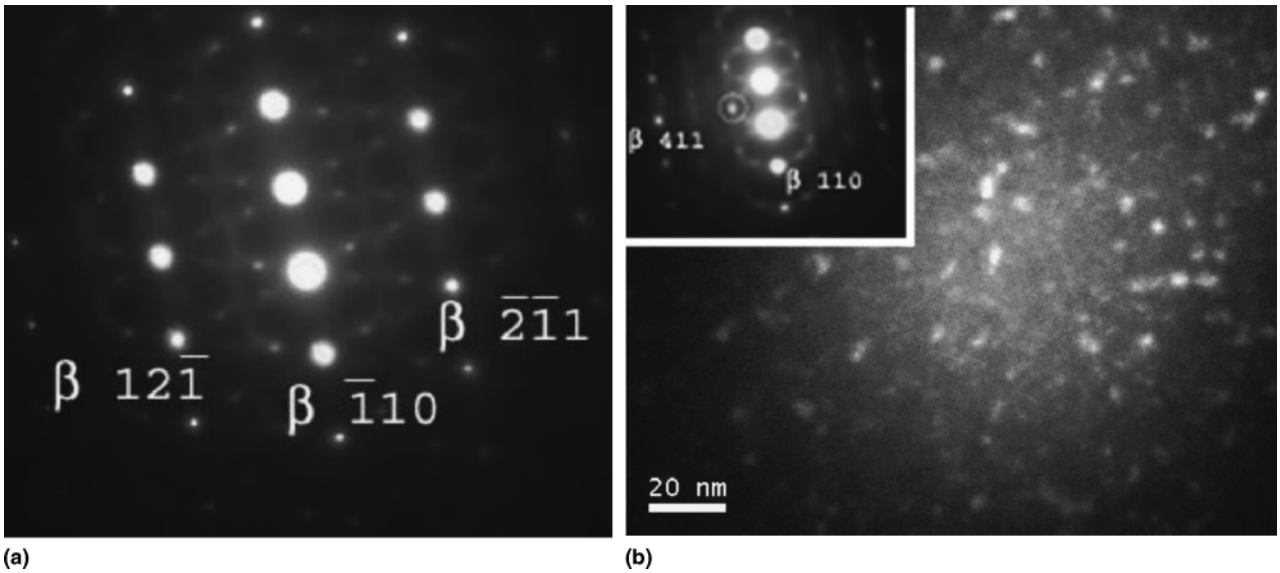

Fig. 8 (a) TEM diffraction pattern obtained with β-near [113] zone axis, (b) dark-field image using ω spot illustrating ω size and distribution-zone axis [122]β

5. Conclusions

The nucleation and growth of the α phase in a two-phase β metastable Ti alloy, the Ti-LCB, were studied after several heat or thermomechanical treatments using light microscopy, SEM, TEM, and EBSD-OIM. The following conclusions can be drawn.

- At high temperature, the precipitation of the α phase is observed at the β grain boundaries as a continuous film that can result from the coalescence of several α grains. These develop the Burgers orientation relationship with respect to one of the adjacent β grains. At lower temperatures, the α phase precipitates as intragranular thin platelets.
- Interrupted aging is also characterized by an intragranular precipitation thanks to the introduction of some precursors during quenching and heating that increase the nucleation rate of the α phase and provide a homogeneous distribution of this phase. This phenomenon is also observed in the case of cold rolling, which strongly increases the density of intragranular α grains. However, this intragranular nucleation hinders the β recrystallization.
- Continuous cooling is characterized by an acicular precipitation of the α phase. The larger β grain size leads to thinner but longer α plates.

Acknowledgments

The work of P.J. Jacques was supported by the Fonds National de la Recherche Scientifique (F.N.R.S.), Belgium. This work was partly supported by the Belgian State, the Prime Minister's Office, the Federal Office for Scientific, Technical and Cultural Affairs within the framework of the PAI P5/P08 project "From Microstructure Towards Plastic Behavior of Single- and Multiphase Materials." The work of A. Lenain was supported by the Fonds pour la formation à la Recherche dans l'Industrie et dans l'Agriculture (F.R.I.A.), Belgium. The authors would like to thank the Fonds de la Recherche Fondamentale Collective d'initiative des chercheurs (F.R.F.C.), for their financial support for the acquisition of the FEG-SEM and EBSD systems, TIMET-Savoie for providing the material, and Techspace Aero.

References

1. G. Lütjering and J.C. Williams, *Titanium,* Springer, B. Derby, Ed., Springer-Verlag, Berlin, Heidelberg, Germany, 2003, p 27-44 and 248-260
2. O. Jin and S. Mall, Effects of Microstructure on Short Crack Growth Behavior of Ti-6Al-2Sn-4Zr-2Mo-0.1Si Alloy, *Mater. Sci. Eng. A,* Vol 359, 2003, p 356-367
3. T.F. Broderick, A.G. Jackson, H. Jones, and F.H. Froes, The Effect of Cooling Conditions on the Microstructure of Rapidly Solidified Ti-6Al-4V, *Metall. Trans. A,* Vol 16, 1985, p 1951-1959
4. Y.G. Li, M.H. Loretto, D. Rugg, and W. Voice, Effect of Heat Treatment and Exposure on Microstructure and Mechanical Properties of Ti-25V-15Cr-2Al-0.2C (Wt.%), *Acta Mater.,* Vol 49, 2001, p 3011-3017
5. C. Sauer and G. Lütjering, Influence of α Layers at the Grain Boundaries on Mechanical Properties of Ti-Alloys, *Mater. Sci. Eng. A,* Vol 319-321, 2001, p 393-397
6. C. Sauer and G. Lüetjering, Thermo-Mechanical Processing of High Strength β-Titanium Alloys and Effects on Microstructure and Properties, *J. Mater. Proc. Technol.,* Vol 117, 2001, p 311-317
7. T. Furuhara, A.M. Dalley, and H.I. Aaronson, Interfacial Structure of Grain Boundary α Allotriomorphs in a Hypoeutectoïd Ti-Cr Alloy, *Scr. Metall.,* Vol 22, 1988, p 1509-1514
8. S. Azimzadeh and H.J. Rack, Phase Transformations in Ti-6.8Mo-4.5Fe-1.5Al, *Metall. Mater. Trans. A,* Vol 29, 1998, p 2455-2466
9. F. Prima, "Etude Métallurgique d'un Nouvel Alliage de Titane β-Métastable," Ph.D. Thesis, Rennes National Institut of Applied Sciences, 2000
10. F. Prima, P. Vermaut, I. Thibon, J. Debuigne, and D. Ansel, A Low Cost Metastable Beta Titanium Alloy: Thermal Treatments, Microstructures and Mechanical Properties, *J. Phys.,* Vol 11, 2001, p 241-248
11. O.M. Ivasishin, P.E. Markovsky, Yu. V. Matviychuk, and S.L. Semiantin, Precipitation and Recrystellization Behavior of Beta Titanium Alloys during Continuous Heat Treatment, *Metall. Mater. Trans. A,* Vol 34, 2003, p 147-158
12. S. Malinov, W. Sha, and P. Markovsky, Experimental Study and Computer Modelling of the $\beta \rightarrow \beta + \alpha$ Phase Transformation in β21s Alloy at Isothermal Conditions, *J. Alloys Compd.,* Vol 348, 2003, p 110-118
13. F.J. Gil, M.P. Ginebra, J.M. Manero, and J.A. Planell, Formation of a-Widmanstätten Structure: Effects of Grain Size and Cooling Rate on the Widmanstätten Morphologies and on the Mechanical Properties in Ti6Al4V, *J. Alloys Compd.,* Vol 329, 2001, p 142-152